An Electronically Steerable Antenna Designed for Accurate DoA Determination of U-NII-2-Extended WLAN Devices

Zasli Afandi Baharuddin[1], Elyas Palantei[2], Intan Sari Areni[3]
Department of Electrical Engineering
Universitas Hasanuddin
Makassar, Indonesia
[1]baharuddinza21d@student.unhas.ac.id
[2]elyas_palantei@unhas.ac.id
[3]intan@unhas.ac.id

Abstract— **Determining the location of the beam source of WLAN devices causing harmful interference to TWDR in the U-NII-2-Extended band requires effective methods and devices. Research regarding the construction of the directional finding antennas in this band is still lacking. An intelligent electronically steerable parasitic array radiatory (ESPAR) antenna design was constructed in this study to perform two critical tasks, i.e., to determine the direction and the location of the radiation source that causes interferences. An electronically beam steerable antenna was implemented in such way using a digitally controlled PE42424 SPDT switch which connected directly to each parasitic element. This allows each parasitic part to stay in one of the two states, i.e., ON or OFF. The RF switch circuit was designed on the plated-through-hole PCB structure. In the ON state, this connects the parasitic elements and the grounding part to reflect the induced RF signal of each element to all OFF-stated parasitic directions. The numerical computation of the designed antenna shows consistent radiation from the main beam pattern which varies at every 45° angle. The maximum gain achieved was up to 8.76 dBi. The reflection coefficient and VSWR obtained through the numerical assessment were -22.3 dB and 1.53, respectively.**

Keywords—Intelligent ESPAR, Steerable Antenna, Direction Finding, TDWR Application, U-NII-2-Extended band, WLAN device, Beam Steering, SPDT RF-switch.

I. INTRODUCTION

The increasing need for internet access, especially at home and in the office, has driven the increase in the use of WLAN device. The most widely use of WLAN devices as a transmission link of the access point operates in the 5 GHz frequency band. However, the use of frequencies in the increasingly dense U-NII-3 band results in interference so that the throughput is also decreased [1]. Therefore, users of WLAN devices often use frequencies other than the U-NII-3 band, such as the U-NII-2-Extended (5470 MHz - 5725 MHz) band. However, this has the potential to cause harmful interference to the Terminal Doppler Weather Radar (TDWR) operating in the C-band [2][3][4][5]. This endangers public safety because of a decrease in the quality of the data obtained by radar imagery which can lead to underestimation or overestimation of weather forecasts for aviation. Dynamic frequency selection (DFS), which is a standard that need to be applied to WLAN devices operating in the 5 GHz frequency band, is not optimal in preventing harmful interference to TDWR [6][7]. In fact, the result of investigations in the field shows that in addition to the failure of the DFS function in several cases, users of WLAN devices have even disabled the DFS function on these devices to operate in U-NII-2-Extended band [4]. Therefore, the emission source's location needs to be identified so the activity that causes harmful interference can be stopped.

Determining the location of the transmitting device for WLAN devices in indoor and outdoor conditions is very different. In an indoor environment, research can be carried out using a handheld device such as a smartphone without an additional antenna [8][9]. This method uses RSS fingerprint crowdsourcing where the determined location is carried out in two phases: the offline phase and the online phase. In the offline phase, a radiomap is made by measuring all reference points (RP) which are then stored in a database. In the online phase, the coordinates of the beam source position are estimated by comparing the measurement results in real time with the fingerprint database obtained in the offline phase [10]. The obtained WLAN fingerprint database is strongly affected by the measurement conditions [11]. Therefore, the changes in the environmental conditions of measurement require updating of the database. Apart from RSS, crowdsourcing fingerprinting can be done using Channel State Information (CSI) [12][13]. In practice, to obtain a better performance, a sub-carrier is selected that is slightly affected by multipath [14]. The crowdsourcing fingerprint method requires large database storage and processing, so this method is not suitable for very dynamic outdoor environment whether it is affected by moving vehicles with WLAN devices on them or landscape changes coupled with the area on a square kilometer scale.

A study uses a smartphone to determine the location of a WLAN devices emission source in an outdoor environment using the doppler technique [15]. This research proposes to use 2.4 GHz since it has a longer range than 5 GHz. Standard antenna gain in smartphone is not adequate to accomplish this task. Therefore, to determine the location of the WLAN devices in an outdoor environment on the 5 GHz band, an additional antenna is required.

In addition to using RF fingerprint crowdsourcing, determining the location of WLAN devices is carried out by using the Time of Arrival (TOA), Time Difference of Arrival (TDOA), Received Signal Strength (RSS) and Angle of Arrival (AoA) techniques [16][17]. The TOA and TDOA techniques require clock synchronization at each monitoring station which raise deployment cost [18]. RSS measurement is the most widely implemented technique due to its lower cost and ease of implementation. The AoA technique only requires a minimum of two measurement angles to estimate the location of the emitting signal. With each of its advantages, the RSS technique can be combined with the AOA technique [19].

979-8-3503-9961-5/22/$31.00 ©2022 IEEE

Research on antennas to determine the location of WLAN devices is generally carried out in the frequency band below 5 GHz and optimized to operate at band 2.4 GHz for indoor or building use [20]-[28]. Prototype antenna array for direction finding initially by using variable capacitance diodes on passive elements for beamforming [20]. In addition to using a varactor, beamforming can be done using a switch. The switch can be a P.I.N diode or SPDT [21][22]. Intelligent antennas in the form of low gain antennas that are arranged linearly are calibrated. Then programming is carried out on the client's beamforming weight value obtained for scanning each angle. By using the triangulation technique indoors, an error resolution of 1 m is obtained with a probability of 0.821 [23]. Another study in the indoor environment showed that the interferometry technique with two antennas combined with OFDM Channel State Information could show DoA with a median error of 8° - 15° [24].

In addition to using antennas with specific characteristics, the direction finding uses algorithms to compute the received signal. The antenna is designed to estimate DoA based on signal strength (RSS) using the Power Pattern Cross Correlation (PPCC) and Support Vector Machine (SVM) algorithm that can provide a precision level of 5° - 7° and 1° - 6° for SNR 30 dB to 0 dB, respectively [26]. In addition, the amplitude and phase parameters obtained from the received IQ signal samples can be used to estimate DoA using the Multiple Signal Classification (MUSIC) algorithm with a better level of precision [21]. This algorithm is based on eigenvalue decomposition so that as a tradeoff, the required computation time is higher [29].

To the author's knowledge, the study of direction finding antenna in the 5 GHz frequency band is only the ESPAR antenna that has been simulated and prototyped for V2X applications at a frequency of 5.89 GHz [19]. The simulation result shows that the maximum gain on the horizontal plane obtained is 2.05 dBi with a precision of 1° - 5° for SNR 20 dB and 0 dB. To receive better signals, especially in outdoor environments, an antenna with a higher gain is needed. The above algorithm can be used in various configurations of ESPAR antennas designed for direction finding. An ESPAR antenna operates in the 5 GHz band using a cavity-backed slot antenna [30]. The antenna is designed for wireless communication systems so that the beam steering only covers 46 degrees in the E plane.

DoA estimation for WLAN devices in the 5 GHz band using conventional WLAN devices is very time consuming and laborious because DoA estimation is done by rotating the directional antenna to find the maximum RSS while moving toward direction that shows an increase in RSS. Using the R&S®ADD207 Compact UHF/SHF DF antenna [31] with the R&S® MobileLocator [32] is very effective for locating the interference source. However, this device is not designed to display the SSID and Mac Address of the signal source. Therefore, an antenna is proposed for an effective direction finding and can be used in estimating the DoA of the emitting source causing harmful interference in the U-NII-2 Extended band with an acceptable level of precision.

In this paper, research is conducted to design a smart antenna to operate in the U-NII-2-Extended band precisely to estimate the DoA of WLAN telecommunication devices that potentially cause interference in TDWR. Radiation patterns with high directivity are required. A novel parameter other than structural parameters in the design of ESPAR antennas that affect the characteristics of ESPAR antennas in the 5 GHz band to obtain a higher gain compared to previous studies [19][34] is proposed. The main contribution of this paper is adjusting the track length between parasitic elements and ground which has a significant impact in increasing the gain ESPAR antenna especially in 5 GHz band.

Simulations are carried out to obtain a low back lobe and side lobe. The antenna is intelligently designed to have a gain of up to 8 dBi so that signal reception can be better than the previously studied ESPAR antennas in the 5 GHz band. SPDT switches are used in this antenna due to the use of variable capacitance diodes and P.I.N. diodes, it is still necessary to regulate the voltage on the switching network to obtain the best antenna performance [20][33]. In the DoA estimation, the designed antenna uses only one RF feed. Therefore, the antenna based on the ESPAR method is simpler and cheaper than the antenna system that uses digital beamforming, which uses a lot of RF feeds.

II. ANTENNA DESIGN FOR DIRECTION FINDING ON U-NII-2-EXTENDED BAND

The smart antenna design is expected to receive signals at whole 360° coverage area. Therefore, this antenna is designed from several elements arranged in a circle. Spatial electromagnetic field coupling between radiating elements forms a radiation pattern. For RF signal processing to carry out faster, only one receiver is used, so it proposes to use one active element in the center of the ground plane with eight parasitic (passive) elements arranged in a circle with a symmetrical configuration. A 45° angle separates the arrangement of the passive monopole elements as in Fig. 1. Therefore, this smart antenna is called a Circular Nine Monopole Element.

As the calculation base, the frequency used in this design is 5.6 GHz because the frequency is in the middle of the U-NII-2-Extended band. In addition, TDWR also operates around this frequency. Therefore, this design is aimed to obtain a wide antenna bandwidth to cover the U-NII-2-Extended band.

The material that is used as an active and passive element is brass, while the dielectric material used is FR-4 with ε = 4.3 and μ = 1.0. The height of the active and passive elements is $\lambda/4$, with the distance between the active and passive elements of $\lambda/2$. The space of active and passive elements is very influential in the formation of the beam. Distance that is too far can result in the beam direction being out of focus according to the passive element configuration. On the other hand, if the distance is too close, the antenna manufacturing process becomes more difficult. Each passive element (P_1, P_2, …., P_8) is connected to the ground using a switch adjacent to the plated through hole (PTH). The

TABLE I. ANTENNA DIMENSION OPTIMIZATION

No	Parameter	Size	Calculation (mm)	Optimized (mm)
1	Monopole element length	$\lambda/4$	12.7	12.3
2	Substrate radius	1.1 λ	55.9	55.9
3	Ground radius	λ	50.9	50.9
4	Distance between active and passive element	$\lambda/2$	25.4	25.4
5	Distance between passive element and PTH	$\lambda/3$	16.9	15.5

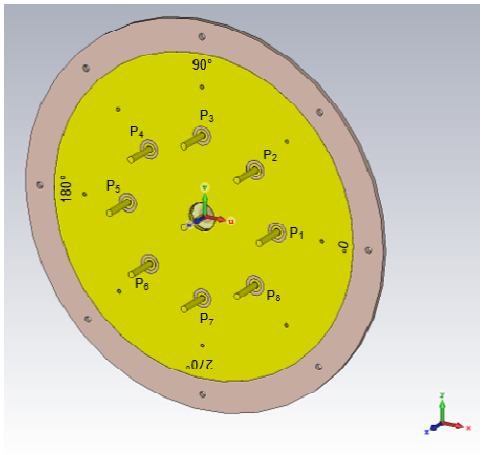

Fig. 1. The proposed antenna layout

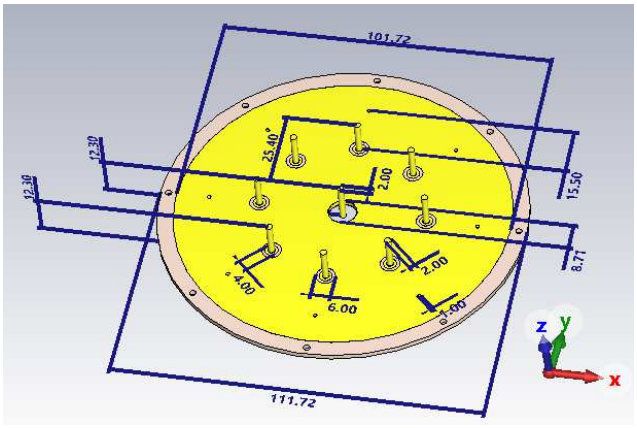

Fig. 2. The optimized antenna dimensions

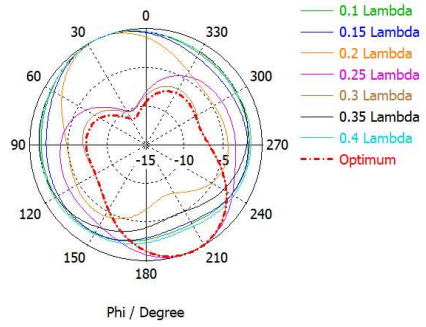

Fig. 3. Normalized directivity for various distance between parasitic elements and PTH

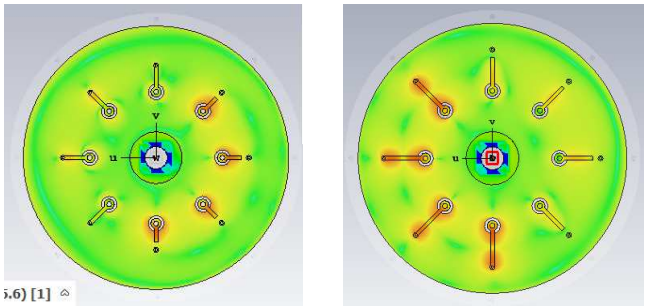

(a) (b)

Fig. 4. Effect of various of distance between passive element on PTH, (a) less than 0.2 λ, (b). more than 0.25 λ

dimensions of the proposed antenna are optimized to obtain the dimensions as in TABLE I. and Fig. 2.

The smart antenna can determine the direction of the beam source based on the RF signal received through the passive element configuration. The beam direction is changed by adjusting the condition of the eight passive elements to the ground plane. The condition is either short or open. To set short and open conditions, SPDT PE42424 is used. The configuration of the passive element condition on the ground plane is carried out using an RF switching circuit based on the signal processing results obtained from the processing unit. By providing a digital signal 1 on the digital control logic input PE42424, the RF signal on the passive element monopole is connected to the ground via the RF1 pin. If a digital signal 0 is given, then the RF signal on the passive element monopole is not connected to the ground because it is connected to the RF2 pin which is left open. The configuration shift of the sorted passive elements is carried out sequentially when the RF signal parameter measurement results are obtained.

III. Computing Results and Discussion

A. Radiation Pattern

Passive element switching is simulated by adjusting the length of the trace connecting the monopole passive element to ground via the PTH to obtain an open or closed path. A short condition is simulated by connecting passive elements to ground, and vice versa.

For each combination of shortened passive elements, a different radiation pattern is produced. The resulting radiation pattern is directed away from the shortened element. The RF signal converges in opposite directions in the trace between the shortened passive elements and the PTH. Therefore, the signal is amplified away from the shortened passive elements. Unlike the open element, the current in the trace between the passive element and the PTH is unidirectional. In other words, a short passive element functions as a reflector, while an open passive element functions as a guide.

The results of the previous research [34] show that the structural parameters in ESPAR antenna design are the number of passive elements, the length of active and passive elements, and the distance between passive and active elements. In this research, the results of the proposed antenna simulation show the distance between passive elements with PTH also affect the radiation pattern (see Fig. 3). At a distance less than 0.2λ, the radiation pattern is towards the shortened because the current from the PTH is higher than the current at the bottom of the shortened passive element, as shown in Fig. 4. (a). While more than 0.25λ-0.35λ, the radiation pattern direction is away from the shortened element because the current from the passive elements and PTH is almost similar but have opposite direction (see Fig. 4. (b)).

The configuration of shortened passive elements required for direction finding use is a configuration that produces a radiation pattern with directivity with a large level difference between the main lobe and the side lobe, and the main lobe and the back lobe. The configuration of these elements is expressed as SxOy, where x represents the number of elements that are shortened, and y represents the number of

TABLE II. DIRECTIVITY AND GAIN IN VARIOUS ANTENNA CONFIGURATIONS

No.	Configuration	Directivity (db)			Gain (dBi)			Main lobe direction	Back lobe/ side lobe direction
		Main lobe	Side lobe / back lobe	Difference	Main lobe	Side lobe / back lobe	Difference		
1	S1O7 [10000000]	6.88182	6.88147	0.00035	6.6576	6.65724	0.00036	103	257
2	S2O6 [11000000]	6.56013	0.422989	6.137141	6.30474	0.167606	6.137134	134	21
3	S3O5 [11000001]	6.9806	1.9788	5.0018	6.640222	1.63842	5.001802	180	46
4	S4O4 [111000001]	9.19906	2.01956	7.1795	8.75745	1.50965	7.2478	203	322
5	S5O3 [11100011]	8.775	1.876	6.899	8.24482	0.785693	7.459127	180	0
6	S6O2 [11110011]	8.04625	1.67343	6.37282	7.4667	1.09389	6.37281	205	25
7	S7O1 [11110111]	6.82671	1.12603	5.70068	6.03	0.329357	5.700643	131	329.5

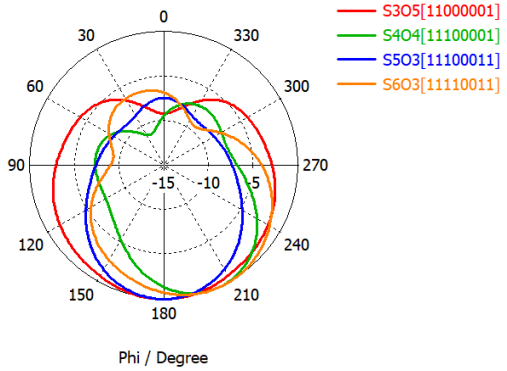

Fig. 5. Smart antenna normalized radiation pattern with 4 different configurations

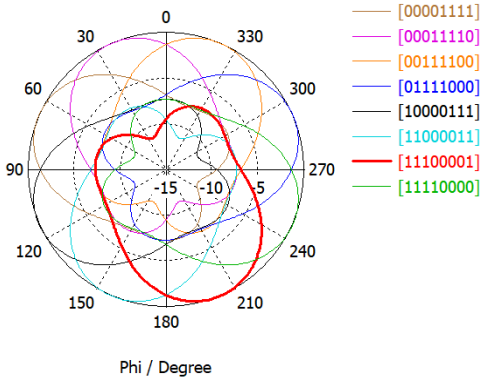

Fig. 6. Smart antenna normalized radiation patter with 8 direction

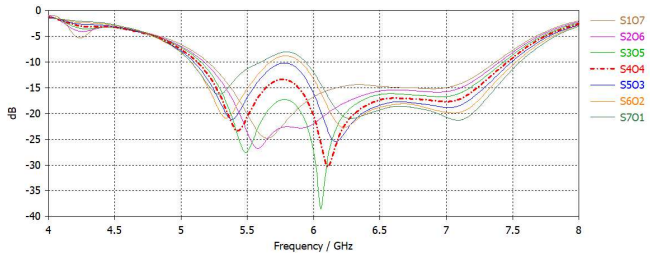

Fig. 7. Reflection coefficient with various configuration

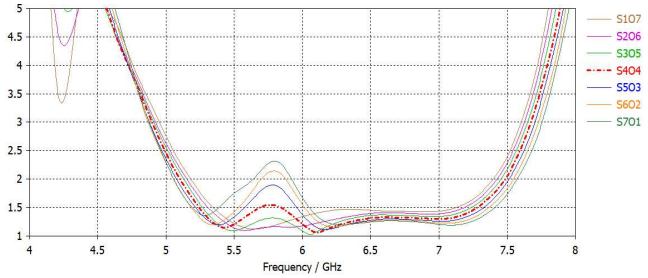

Fig. 8. VSWR with various configuration

open elements. Shortened P_N element is denoted by 1 while open elements are denoted by 0. Fig. 5 shows the radiation pattern of the simulation results for each combination of shortened passive elements. Each passive element configuration produces a different radiation pattern. The radiation pattern for the S1O7, S2O6, and S7O1 configurations are not shown in the figure since the radiation pattern produced has side lobe or back lobe that is almost the same size as the main lobe, while the other configurations radiate small side lobe and back lobe. In contrast, the other configurations radiate the small size of back lobe and side lobe.

To perform a 360° scan horizontally, a shift in the configuration of the short and open elements is performed. Each shift in the configuration of the shortened element will result in a shift in the direction of the main lobe by approximately 45° as shown in Fig. 6.

B. Reflection Coefficient, VSWR, and Bandwidth

In Fig. 7, the reflection coefficient of the proposed antenna simulation shows that the configuration with 1 to 5 shortened elements meet the criteria below -10 dB in the required band. Changing the configuration of the passive element of the antenna produces a significant deviation of the reflection coefficient because each configuration produces a different current distribution in the passive element and its impact on the input impedance of the antenna [35]. For example, the value of the reflection coefficient of the antenna with the S4O4 configuration at a frequency of 5.47 GHz is -22.30 and increases to -13.56 at a frequency of 5.725 GHz. Whereas, in antenna configurations with 6 and 7 shortened

TABLE III. COMPARATIVE PERFORMANCE OF ESPAR ANTENNA

No	Freq (GHz)	Max. Gain (dBi)	VSWR	Coverage	Ref.
1	0.923	8.52	<1.92	360°, step size 60°	[36]
2	1.8, 1.9, 2.3, 2.4, 2.5	7.37	<2	360°, step size 60°	[37]
3	2.484	7.5	-	360°, step size 45°	[27]
4	2.4-2.5	11.4	-	360°, step size 45°	[28]
5	2.45	5.1	-	360°, step 30°	[38]
6	5.1-5.3	6.05	-	46° (from -26° to 20°)	[30]
7	5.89	2.05	-	360°, step size 30°	[19]
8	5.47 – 5.725	8.76	<1.54	360°, step size 45°	This

elements, the reflection coefficient does not meet the criteria some of desired frequency band.

The simulation results show that in the frequency range of 5.470 - 5725 GHz, the VSWR value for configurations with 1 to 4 elements is shortened, the VSWR value is < 1.54, while in the S503 combination, the VSWR value is < 1.85. The VSWR values obtained in different configurations are shown in Fig. 8.

The bandwidth obtained based on the simulation results in the configuration of 1 element to 5 shortened elements is about 2.3 GHz. In the S6O2 and S7O1 configurations, the reflection coefficient values at a frequency of 5.6 GHz are above -10 dB. Therefore, these configurations cannot be used.

C. Gain and Directivity

The radiation pattern that produces the highest directivity with the maximum difference between the main lobe, side lobe, and back lobe is obtained in the S4O4 configuration where four passive elements are shortened (switching ON) and four are open (switching OFF). The maximum gain and directivity for each radiation pattern can be seen in TABLE II. The simulation results show that the configuration with the difference in the number of short and open elements results in a lower gain and lower directivity, because the emitted RF signal does not point in one direction.

Comparison results of the performance analysis of the proposed antenna with the previous ESPAR antenna research is shown in TABLE III. In 5 GHz band the previous research did not achieve a gain of 7 dBi as is commonly obtained in 2.4 GHz band and below. Most of the research results we compared used passive elements connected to a circuit switch directly connected to ground on the opposite side via a via. The use of 0.305 λ track between parasitic element and ground, reflects the induced RF signal well so that a higher gain is obtained.

IV. CONCLUSION

The circular configuration of the nine-monopole elements intelligent ESPAR antenna has been designed to operate on the U-NII-2-Extended band. By optimizing track length between parasitic element and PTH ground antenna at 0.305 λ, the antenna produced a radiation pattern that has a gain of more than 8 dBi. Those optimum gain were obtained by setting-up 4 or 5 parasitic elements to be shortened (meaning 4 or 5 elements connected to grounding plane), respectively. Under these configurations, significant impacts were also encountered on the coefficient reflection and VSWR values. This antenna design could cover 360° angle direction reception with eight steps in the horizontal plane (every step ~ 45° angle). The simulation results show that the proposed antenna has the excellent performance parameters that can be used to locate WLAN devices in the U-NII-2-Extended band. Due to the very compact dimensions of the antenna design, this antenna allows it to be implemented in handheld use or mounted on a car.

ACKNOWLEDGMENT

The authors would like to thank the Ministry of Communications and Informatics, Republic of Indonesia, for the sufficient research funding which support the implementation of the whole R&D project activities.

REFERENCES

[1] I. Dolińska, M. Jakubowski and A. Masiukiewicz, "Interference comparison in Wi-Fi 2.4 GHz and 5 GHz bands," *2017 International Conference on Information and Digital Technologies (IDT)*, 2017, pp. 106-112, doi: 10.1109/DT.2017.8024280.

[2] A. L. Brandao, J. Sydor, W. Brett, J. Scott, P. Joe and D. Hung, "5 GHz RLAN interference on active meteorological radars," *2005 IEEE 61st Vehicular Technology Conference*, 2005, pp. 1328-1332 Vol. 2, doi: 10.1109/VETECS.2005.1543524.

[3] B. D. Cordill, S. A. Seguin and L. Cohen, "Electromagnetic interference to radar receivers due to in-band OFDM communications systems," *2013 IEEE International Symposium on Electromagnetic Compatibility*, 2013, pp. 72-75, doi: 10.1109/ISEMC.2013.6670384.

[4] Electronic Communications Commitee, ECC Report 192 The Current Status of DFS (Dynamic Frequency Selection) In the 5 GHz Frequency Range, 2014.

[5] Ministry of Communications and Informatics of Republic of Indonesia, Data Statistik Direktorat Jenderal Sumber Daya dan Perangkat Pos dan Informatika 2020, 2021, Bogor: IPB Press.

[6] S. P. Sone, J. Lehtomäki, Z. Khan, K. Umebayashi and Z. Javed, "Proactive Radar Protection System in Shared Spectrum via Forecasting Secondary User Power Levels," in *IEEE Access*, vol. 10, pp. 40367-40380, 2022, doi: 10.1109/ACCESS.2022.3166844.

[7] Z. Horváth and D. Varga, "Elimination of RLAN interference on weather radars by channel allocation in 5 GHz band," *2009 International Conference on Ultra Modern Telecommunications & Workshops*, 2009, pp. 1-6, doi: 10.1109/ICUMT.2009.5345374.

[8] J. Xue, J. Liu, M. Sheng, Y. Shi and J. Li, "A WiFi fingerprint based high-adaptability indoor localization via machine learning," in *China Communications*, vol. 17, no. 7, pp. 247-259, July 2020, doi: 10.23919/J.CC.2020.07.018.

[9] J. Choi, G. Lee, S. Choi and S. Bahk, "Smartphone Based Indoor Path Estimation and Localization Without Human Intervention," in *IEEE Transactions on Mobile Computing*, vol. 21, no. 2, pp. 681-695, 1 Feb. 2022, doi: 10.1109/TMC.2020.3013113.

[10] P. Ssekidde, O. Steven Eyobu, D. S. Han, and T. J. Oyana, "Augmented CWT Features for Deep Learning-Based Indoor Localization Using WiFi RSSI Data," Applied Sciences, vol. 11, no. 4, p. 1806, Feb. 2021, doi: 10.3390/app11041806.

[11] A. Yassin et al., "Recent Advances in Indoor Localization: A Survey on Theoretical Approaches and Applications," in *IEEE Communications Surveys & Tutorials*, vol. 19, no. 2, pp. 1327-1346, Secondquarter 2017, doi: 10.1109/COMST.2016.2632427.

[12] N. Singh, S. Choe and R. Punmiya, "Machine Learning Based Indoor Localization Using Wi-Fi RSSI Fingerprints: An Overview," in *IEEE Access*, vol. 9, pp. 127150-127174, 2021, doi: 10.1109/ACCESS.2021.3111083.

[13] X. Wang, L. Gao, S. Mao and S. Pandey, "CSI-Based Fingerprinting for Indoor Localization: A Deep Learning Approach," in *IEEE Transactions on Vehicular Technology*, vol. 66, no. 1, pp. 763-776, Jan. 2017, doi: 10.1109/TVT.2016.2545523.

[14] T. F. Sanam and H. Godrich, "An Improved CSI Based Device Free Indoor Localization Using Machine Learning Based Classification Approach," *2018 26th European Signal Processing Conference (EUSIPCO)*, 2018, pp. 2390-2394, doi: 10.23919/EUSIPCO.2018.8553394.

[15] Y. -Y. Shih, A. -C. Pang and P. -C. Hsiu, "A Doppler Effect Based Framework for Wi-Fi Signal Tracking in Search and Rescue Operations," in *IEEE Transactions on Vehicular Technology*, vol. 67, no. 5, pp. 3924-3936, May 2018, doi: 10.1109/TVT.2017.2752766.

[16] N. Saeed, H. Nam, T. Y. Al-Naffouri and M. -S. Alouini, "A State-of-the-Art Survey on Multidimensional Scaling-Based Localization Techniques," in *IEEE Communications Surveys & Tutorials*, vol. 21, no. 4, pp. 3565-3583, Fourthquarter 2019, doi: 10.1109/COMST.2019.2921972.

[17] S. M. Asaad and H. S. Maghdid, "A Comprehensive Review of Indoor/Outdoor Localization Solutions in IoT era: Research Challenges and Future Perspectives," Computer Networks, vol. 212, p. 109041, Jul. 2022, doi: 10.1016/J.COMNET.2022.109041.

[18] W. Ding, Q. Zhong, Y. Wang, C. Guan, and B. Fang, "Target Localization in Wireless Sensor Networks Based on Received Signal Strength and Convex Relaxation," *Sensors*, vol. 22, no. 3, p. 733, Jan. 2022, doi: 10.3390/s22030733.

[19] D. Duraj, M. Rzymowski, K. Nyka and L. Kulas, "RSS-Based DoA Estimation Using ESPAR Antenna for V2X Applications in 802.11p Frequency Band," *2020 14th European Conference on Antennas and Propagation (EuCAP)*, 2020, pp. 1-5, doi: 10.23919/EuCAP48036.2020.9135688.

[20] T. Ohira and K. Gyoda, "Hand-held microwave direction-of-arrival finder based on varactor-tuned analog aerial beamforming," *APMC 2001. 2001 Asia-Pacific Microwave Conference (Cat. No.01TH8577)*, 2001, pp. 585-588 vol.2, doi: 10.1109/APMC.2001.985441.

[21] P. Kwapisiewicz, M. Groth, M. Rzymowski and L. Kulas, "SDR-Based DoA Estimation Using ESPAR Antennas with Simplified Beam Steering," *2019 13th European Conference on Antennas and Propagation (EuCAP)*, 2019, pp. 1-4.

[22] L. Kulas, "Simple 2-D Direction-of-Arrival Estimation Using an ESPAR Antenna," in *IEEE Antennas and Wireless Propagation Letters*, vol. 16, pp. 2513-2516, 2017, doi: 10.1109/LAWP.2017.2728322.

[23] C. -H. Lim, Y. Wan, B. -P. Ng and C. -M. S. See, "A Real-Time Indoor WiFi Localization System Utilizing Smart Antennas," in IEEE Transactions on Consumer Electronics, vol. 53, no. 2, pp. 618-622, May 2007, doi: 10.1109/TCE.2007.381737.

[24] A. Tzur, O. Amrani, and A. Wool, "Direction Finding of rogue Wi-Fi access points using an off-the-shelf MIMO–OFDM receiver," *Physical Communication*, vol. 17, pp. 149–164, Dec. 2015, doi: 10.1016/J.PHYCOM.2015.08.010.

[25] Y. -H. Lee and C. -S. Lin, "WiFi Fingerprinting for Indoor Room Localization Based on CRF Prediction," *2016 International Symposium on Computer, Consumer and Control (IS3C)*, 2016, pp. 315-318, doi: 10.1109/IS3C.2016.89.

[26] M. Tarkowski and L. Kulas, "RSS-Based DoA Estimation for ESPAR Antennas Using Support Vector Machine," in *IEEE Antennas and Wireless Propagation Letters*, vol. 18, no. 4, pp. 561-565, April 2019, doi: 10.1109/LAWP.2019.2891021.

[27] M. Burtowy, M. Rzymowski and L. Kulas, "Low-Profile ESPAR Antenna for RSS-Based DoA Estimation in IoT Applications," in IEEE Access, vol. 7, pp. 17403-17411, 2019, doi: 10.1109/ACCESS.2019.2895740.

[28] Md. M. Rahman and H.-G. Ryu, "IoT Sensor Network Using ESPAR Antenna Based on Beam Scanning Method for Direction Finding," *Sensors*, vol. 22, no. 19, p. 7341, Sep. 2022, doi: 10.3390/s22197341.

[29] N. M. Balamurugan, S. Mohan, M. Adimoolam, A. John, T. reddy G, and W. Wang, "DOA tracking for seamless connectivity in beamformed IoT-based drones," *Computer Standards & Interfaces*, vol. 79, p. 103564, Jan. 2022, doi: 10.1016/J.CSI.2021.103564.

[30] W. Ouyang and X. Gong, "An Electronically Steerable Parasitic Array Radiator (ESPAR) Using Cavity-Backed Slot Antennas," in *IEEE Antennas and Wireless Propagation Letters*, vol. 18, no. 4, pp. 757-761, April 2019, doi: 10.1109/LAWP.2019.2902037.

[31] Rohde & Schwarz, "R&S®ADD207 Compact UHF/SHF DF antenna", https://www.rohde-schwarz.com/us/products/aerospace-defense-security/compact-single-channel/rs-add207-compact-uhf-shf-df-antenna_63493-11903.html, visited on Oct. 10, 2022.

[32] Rohde & Schwarz, "R&S®MobileLocator", https://www.rohde-schwarz.com/us/products/aerospace-defense-security/radiomonitoring-software/rs-mobilelocator_63493-113986.html, visited on Oct. 10, 2022.

[33] E. Palantei and D.V. Thiel, "The Impact of Bias Voltage on the Performance of a P.I.N. Diode Loaded Smart Antenna," Journal of the Japan Society of Applied Electromagnetics and Mechanics (JSAEM), vol.15, no.3, pp.274-277, September 2007.

[34] K. Gyoda and T. Ohira, "Design of electronically steerable passive array radiator (ESPAR) antennas," *IEEE Antennas and Propagation Society International Symposium. Transmitting Waves of Progress to the Next Millennium. 2000 Digest. Held in conjunction with: USNC/URSI National Radio Science Meeting (C*, 2000, pp. 922-925 vol.2, doi: 10.1109/APS.2000.875370.

[35] D. K. Rongas, A. S. Paraskevopoulos, L. D. Marantis, and A. G. Kanatas, "An Integrated Shark-Fin Reconfigurable Antenna for V2X Communications," *Progress in Electromagnetics Research C*, vol. 100, pp. 1-16, 2020, doi:10.2528/PIERC19112005.

[36] Mainsuri et al., "A 923 MHz Steerable Antenna for Low Power Wide Area Network (LPWAN)," *2020 IEEE International Conference on Communication, Networks and Satellite (Comnetsat)*, 2020, pp. 246-250, doi: 10.1109/Comnetsat50391.2020.9328990.

[37] Q. Liang, B. Sun, G. Zhou, and J. Li, "Broadband ESPAR Antenna Using Sleeve Wires," *International Journal of RF and Microwave Computer-Aided Engineering*, vol. 28, no. 9, Nov. 2018, doi: 10.1002/mmce.21410.

[38] M. Czelen, M. Rzymowski, K. Nyka and L. Kulas, "Miniaturization of ESPAR Antenna Using Low-Cost 3D Printing Process," *2020 14th European Conference on Antennas and Propagation (EuCAP)*, 2020, pp. 1-4, doi: 10.23919/EuCAP48036.2020.9135382.